Desalination and Water Treatment
www.deswater.com

doi: 10.5004/dwt.2022.28027

246 (2022) 166–173
January

Low-cost composite ultrafiltration membrane made from TiO_2 and nanocomposite clay materials over zeolite support for oily wastewater purification and heavy metals removal

Wala Aloulou, Hajer Aloulou, Raja Ben Amar*

Chemistry Department, Faculty of Science of Sfax, University of Sfax, Tunisia, emails: walaaloulou6@gmail.com (W. Aloulou), hajer.aloulou89@yahoo.fr (H. Aloulou), benamar.raja@yahoo.com (R. Ben Amar)

Received 1 June 2021; Accepted 4 December 2021

ABSTRACT

A novel composite ultrafiltration membrane Sm-Ti/Z 3 was developed by deposition of active layer made from 70% of TiO_2/Smectite nanocomposite (Sm NC) and 30% commercial TiO_2 nanoparticles (Ti NP) on ceramic zeolite support previously prepared, using the layer-by-layer technique. The characteristics and the morphology of the membrane sintered at 900°C were determined by Brunauer–Emmett–Teller and scanning electron microscopy. A membrane without cracks and showing homogeneous surface and good adhesion on the support was achieved. The characteristics of the membrane were a mean pore diameter of 16 nm and a water permeability of 95 L/h m^2 bar. The application of this membrane to the purification of oily effluent shows good performance in terms of permeate flux and pollutants removal with almost total retention of chemical oxygen demand, oil and turbidity. In addition, Sm-Ti/Z 3 membrane displayed an important removal of the conductivity beyond 46%. This result is explained by the high elimination of heavy metals (>96%) such as copper, plumb and zinc. The performances of the new membrane suggest also its potential application for remediation of oily wastewater contaminated with heavy metals.

Keywords: Titania-smectite nanocomposite; Titania nanoparticles; Zeolite support; Ultrafiltration membrane; Oily wastewater; Heavy metals

1. Introduction

In the last years, the pollution of water was a major global problem due to the rapid increasing population and industrialization [1]. Among the pollutants released into the environment, oil has been detected in surface water, groundwater and urban wastewater. Usually, high quantity of industrial oil-contaminated wastewater is generated by pharmaceutical, metallurgical and petrochemical industries resulting in environmental pollution that causes danger to human health directly or indirectly through the food chain and generates ecological problems [2–4]. In particular, wastewater produced from the electroplating industry, generally contains a mixture of oil and heavy metals that need to be treated before it can be discharged to the environment.

Various methods have been investigated to treat wastewater loaded in organic and mineral pollutants such as oil and heavy metals. Conventional purification methods such as air flotation [5,6], gravity separation and skimming [7], centrifugation [8], sand filtration [9], coagulation–flocculation [10], adsorption [2,11,12], or chemical destabilization [13–15] have some disadvantages like high operation cost, corrosion, low efficiency and recontamination problems [16]. In addition, the majority of these methods cannot eliminate the micron and submicron sized oil droplets efficiently [17,18]. Therefore, the development of efficient methods to treat oily wastewater has great interest. Among the promising methods used for the purification of such wastewater, membrane processes such as microfiltration [1,19,20], ultrafiltration [21,22], nanofiltration [23,24]

* Corresponding author.

or reverse osmosis [25] can be utilized to increase purification performances.

Membrane technology is usually used in wastewater treatment since it can be simply integrated and scaled up. In addition, this process has high removal efficiency and relatively low operating cost [24]. Especially, ceramic membranes present particular advantages in the oil/water purification because of their excellent mechanical, chemical and thermal properties [26]. In general, ceramic membranes show a resistance to extreme backwashing and aggressive chemical cleaning during application. Nevertheless, the majority of commercial ceramic membranes is based on expensive high-purity ceramic materials, such as titania, alumina, zirconia and need high sintering temperature which increases the ceramic membrane cost [27,28]. Consequently, the minerals ceramic membranes have attracted more attention to develop low cost ceramic membranes [29].

Several researchers have studied the efficiency of the ceramic membranes on the purification of the oily wastewater. In this context, Madaeni et al. [30] successfully removed oil from petrochemical effluent by microfiltration membrane based on gamma-Al_2O_3. Wu et al. [31] treated oil/water emulsion containing 200 mg/L oil in the presence of ethanol as additive and found that 95.3% of oil rejection was achieved using a microfiltration carbon membrane. On the other hand several membrane processes have been used by Aloulou et al. [26] for the purification of oily wastewater including microfiltration, ultrafiltration and air gap membrane distillation processes. Almost total oil retention was observed with interesting permeate flux up to 100 L/h m^2. In the same context, Hu et al. [20] tested a new alumina microfiltration membrane modified with graphen oxide for the separation of oily effluent and found that a maximum oil rejection of 98.1% was achieved when the steady permeate flux was reached.

This study aims to develop new ultrafiltration (UF) membrane by directly deposition of nanocomposites (NC) made from a mixture 70% of TiO_2/Smectite nanocomposite (Sm NC) and 30% commercial TiO_2 nanoparticles (Ti NP) on tubular zeolite support by layer-by-layer technique. The NC was selected as active layer for its low cost and antifouling property [32].

The simultaneous high removal of heavy metals (>96%) and oil (>99%) from industrial oily wastewater by this new ceramic membrane represents the novelty of this work.

2. Experimental

2.1. Materials

The nanocomposite TiO_2/smectite (Sm NC) (mean particle size in the range of 8–12 nm) was previously prepared via colloidal route by incorporating titanium(IV) isopropoxide with in the organophilic smectite grains and was described in our previous study [33].

Commercial nanoparticles (Ti NP) of titanium dioxide (TiO_2) of 22 nm, 95% anatase was purchased from Sigma-Aldrich.

Tubular zeolite support of 150 mm of length, 5 mm of inner diameter, with 0.55 μm pore size and 43.7% porosity was previously developed in our laboratory [34].

2.2. Membrane preparation and characterization

Three nanocomposites (NC) based on synthetic nanoparticles (Sm NC) and commercial nanoparticles (Ti NP) at different percentages were utilized for the preparation of three ultrafiltration membranes (UF): Sm-Ti/Z 1 (95% Sm NC – 5% Ti NP); Sm-Ti/Z 2 (85% Sm NC – 15% Ti NP); Sm-Ti/Z 3 (70% Sm NC – 30% Ti NP) via layer-by-layer deposition technique [32].

At first, the inner surface of the tube was cleaned with sand paper to create roughness for easier adhesion between the coating layer and the support. Then, the tube was rinsed with hot of distilled water to eliminate the dust particles. After air drying, it was kept in oven for 24 h at 100°C for excess water removal. Then, 2 wt.% of NC powder was added to 30 wt.% of polyvinyl alcohol solution under constant magnetic stirring [32,33]. The support was coated using layer-by-layer method which was described in our previous study. After drying for 24 h at room temperature, the membrane was sintered at 900°C for 3 h according a heating rate of 2°C/min to simultaneously achieve consolidation of membrane structure and ensure the adhesion between different layers [33].

The membrane morphology and texture were checked by scanning electron microscopy (SEM) (Carl Zeiss MERLIN microscope, Germany). Pore size distribution of the filtration layer was determined from nitrogen adsorption/desorption isotherm (Micromeritics ASAP 2020, USA). Pore diameter was estimated via the BJH (Barrett-Joyner-Halenda) model [35].

2.3. Performance of different membranes via ultrafiltration process

2.3.1. Permeability test and membrane regeneration

Permeability tests were performed using a home-made plant [36] at ambient temperature and at transmembrane pressure (TMP) ranged between 3 and 7 bar. Regeneration of the membrane was approved by back-flushing procedure for 15 min, followed by basic (NaOH 2% at 80°C) and acidic (nitric acid 2% at 60°C) treatment for 20 min. After that, the membrane was rinsed with water until neutral pH. The success of the cleaning procedure was confirmed by measuring the water permeability after the cleaning cycle.

2.3.2. Effluent characterization

The oily effluent was collected from an electroplating industry located in Sfax (Tunisia). Raw and treated wastewaters were analyzed for the determination of the physicochemical characteristics to evaluate the pollutants removal. Conductivity and pH measurements were done by a conductometer (ISTEK EC-400L, USA) and a pH-meter (ISTEK pH-220L, Japan), respectively. Turbidity was measured using a turbidimeter (Hach RATIO 2100A, USA) in accordance with standard method 2130B. Chemical oxygen demand (COD) was estimated by colorimetric method (Fisher Bioblock Scientific reactor COD 10119, Japan). The content of high metals and the oil removal were determined respectively by atomic absorption spectroscopy (AAS) (Perkin Elmer A Analyst 200) and UV-spectrophotometer

at λ = 363 nm. The pollutants retention R through the membrane was calculated according to the following equation:

$$R(\%) = \left(1 - \left(\frac{C_p}{C_f}\right) \times 100\right) \quad (1)$$

where C_f and C_p represent the concentration of pollutants in the feed and in the permeate, respectively. The viscosity of the raw effluent before and after heating process was measured by a rotary viscosimeter Tve-05 (LAMY).

2.3.3. Fouling study

The membrane fouling resistance ability was evaluated by the determination of the permeate flux decay ratio (FDR) in the absence and the presence of heating:

$$\text{FDR} = \frac{J_w - J_s}{J_w} \times 100 \quad (2)$$

where J_w is the water flux of the new membrane and J_s is the stabilized permeate flux during the UF using oily effluent.

3. Results and discussion

3.1. Membranes characterization

3.1.1. Membrane morphology

Surface and cross-section morphologies, given by SEM, for the different NC ultrafiltration membranes sintered at 900°C/3h, Sm-Ti/Z 1, Sm-Ti/Z 2 and Sm-Ti/Z 3, are shown in Fig. 2. It can be clearly observed that all membranes have homogenous surface with the absence of any cracks. The photos of the cross-section shown in Fig. 1a, c, and e related respectively to Sm-Ti/Z 1, Sm-Ti/Z 2 and Sm-Ti/Z 3, prove the good adhesion between the ultrafiltration layer and the support.

For all membranes, it is clear that the slip allows a sufficient flow of the suspension in the support without deep infiltration, which favorite the formation of an ultrafiltration layer. The thickness of the obtained active layer for the three membranes was 0.88, 1.8 and 3 μm for UF1, UF2 and UF3, respectively (Fig. 1b, d and f).

Based on UF membranes characteristics achieved by SEM analysis and the results found in previous works for the development of membrane made from Sm NC doped with Ti NP over silty marls support, proving that the smallest pore size was observed with the composition of 30% Ti NP [32], Sm-Ti/Z 3 membrane with a content of 30% (Ti NP) was selected as the most suitable for this study.

3.1.2. Pore size determination

Ultrafiltration membrane pore size was determined using N_2 adsorption/desorption isotherm at 77 K (Fig. 2a). Results show that the new membrane exhibits a type IV adsorption isotherm according to IUPAC, which is associated with mesoporous structure.

Fig. 2b presents the pore size distribution of the Sm-Ti/Z 3 ultrafiltration membrane sintered at 900°C/3 h. The mean pore diameter was centered at 16 nm. This value confirms again the ultrafiltration domain.

3.1.3. Determination of the water permeability

The permeability of the Sm-Ti/Z 3 ultrafiltration membrane was determined using distilled water (Fig. 3). It can be noticed that the water flux increases linearly with increasing the applied TMP, according to Darcy's law [37]. The membrane permeability was found as 95 L/h m^2 bar.

3.2. Performance during purification of oily wastewater

3.2.1. Application to ultrafiltration treatment

The performance of the new Sm-Ti/Z 3 membrane applied to the oily effluent purification was determined at a TMP of 3 bar and two temperatures of 25°C and 60°C. The evolution of the permeate flux with time achieved during 90 min of filtration shows a progressive decrease of the permeate flux during the first hour for both temperatures and then a stabilization at 50 L/h m^2 at 25°C and 146 L/h m^2 at 60°C (Fig. 4).

This trend might be related to the accumulation of the rejected pollutants on the membrane surface. The fouling study for Sm-Ti/Z 3 membrane used for oily removal was evaluated by determining the FDR fouling parameter. Generally, the lower FDR values given by the percentage flux decays during the filtration are more favorable [38]. Therefore, the heating process was most beneficial for the purification of oily effluent in relation to the obtained values, where FDR decreased from 84.48% at 25°C to 54.69% at 60°C (Fig. 5). The enhancement of permeate flux by 65.75% when the temperature increased from 25°C to 60°C is attributed to the decrease in the viscosity of the effluent from 2.84 × 10^{-3} Pa·s at 25°C to 1.5 × 10^{-3} Pa·s at 60°C leading to an improvement in matter transfer. Therefore, the suitable temperature for the purification of oily effluent was selected as 60°C. It is worthy to notice that this temperature corresponds to that of the raw oily effluent produced during the activity of the company (between 60°C and 70°C).

Table 1 gives the main characteristics of the raw and treated effluents. The performance of the membrane was monitored by measuring the retention rate of the different pollutants in terms of conductivity, turbidity, COD and oil content. Fig. 6 shows a COD retention of 93% and almost total retention in turbidity and oil at a pressure of 3bar. In addition, a decrease in conductivity around 45% was observed.

To better explore the reduction of the conductivity, the estimation of the content in high metals before and after treatment was evaluated (Table 2). It can be noticed that high retention of copper, plumb and zinc, exceeding 96% was observed. This result is similar to that obtained by Puasa et al. [10] using coagulation–flocculation process where 99% of heavy metals retention was observed.

3.2.2. Fouling behavior

The membrane fouling is caused in general by organic or inorganic compounds, bacteria, colloids, or suspended solids. Fouling could decrease the permeate flux and affect the retention of numerous compounds. It can be reversible

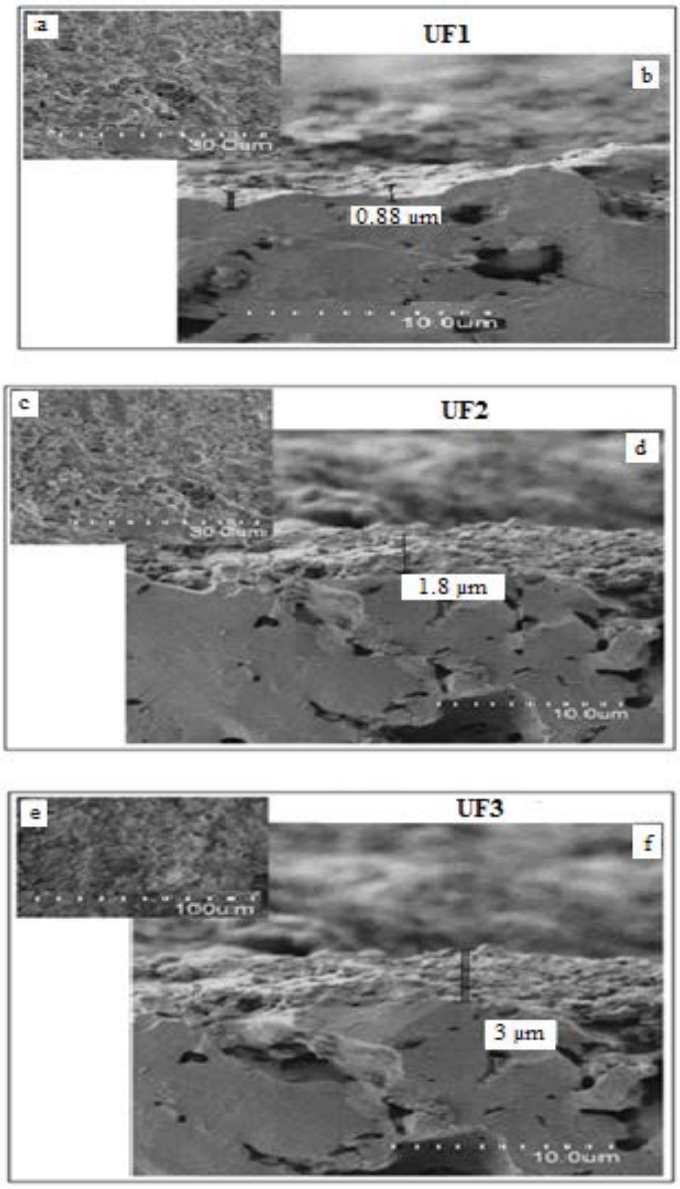

Fig. 1. SEM micrographs of different membranes sintered at 900°C: surface (a, c and e) and cross-section (b, d and f).

or irreversible. Reversible fouling can be eliminated by simple water rinsing or varying some experimental parameters, whereas irreversible fouling is difficult to remove and need chemical cleaning [39].

Previous work has shown that a decrease in the permeate flux can reach up to 18% and 26%–46% due to the presence of reversible and irreversible fouling, respectively [40]. The total resistance (R_T) is the sum of three contributions:

$$R_T = R_m + R_{irrev} + R_{rev} \quad (3)$$

where R_m represents the inherent hydraulic resistance of a clean membrane. R_{rev} results from the concentration polarization and deposition of retained substances on the membrane surface. R_{irrev} results from the contributions of the fouling (adsorption onto the membrane pores and surface).

A specific cleaning is needed to found the initial performances of the membrane. In our case, the different resistance values of the Sm-Ti/Z 3 membrane are illustrated in Table 3. It can be observed that R_{irrev} is higher than R_{rev} and therefore the permeate flux decline is mainly due to the membrane pore fouling and gel formation at the membrane surface which prevent the passage of the oil particles and high metals through the membrane.

3.2.3. Membrane regeneration

The application of the Sm-Ti/Z 3 membrane to the purification of wastewater is often limited by the inevitable fouling, which decreases the membrane performances. The fouling phenomenon is due generally to the hydrophilic–hydrophobic interactions between permeates and membrane surface [41]. The hydrophobic membrane fouling

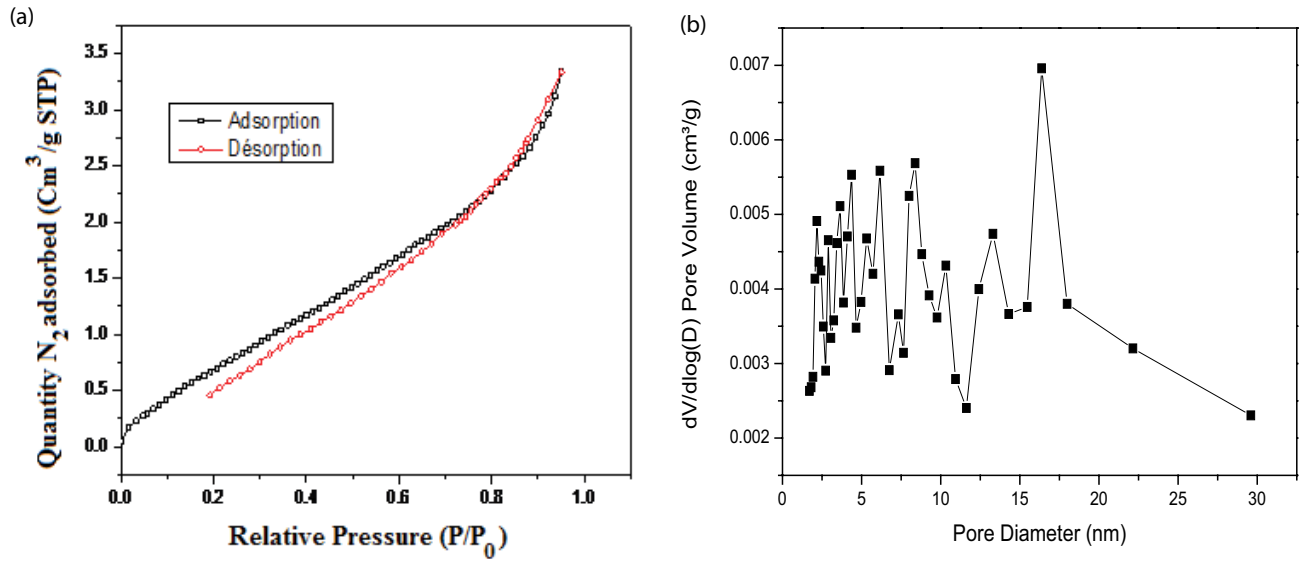

Fig. 2. Nitrogen adsorption–desorption of Sm-Ti/Z 3 membrane: isotherm (a) and pore size distribution (b).

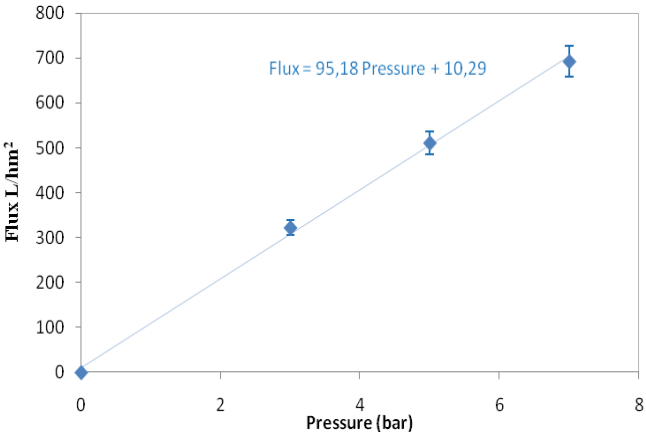

Fig. 3. Water permeability of Sm-Ti/Z 3 membrane.

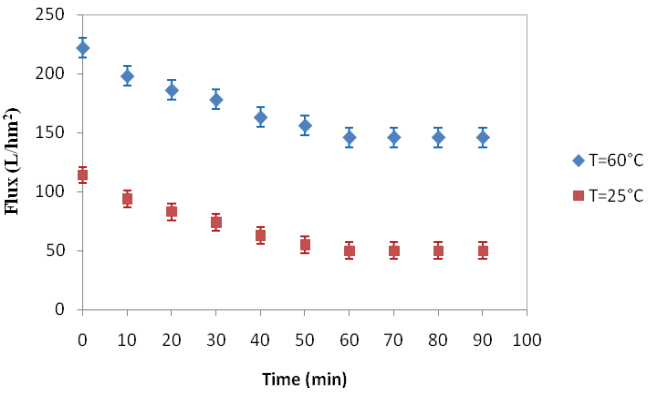

Fig. 4. Permeate flux vs. time at different temperatures using Sm-Ti/Z 3 membrane.

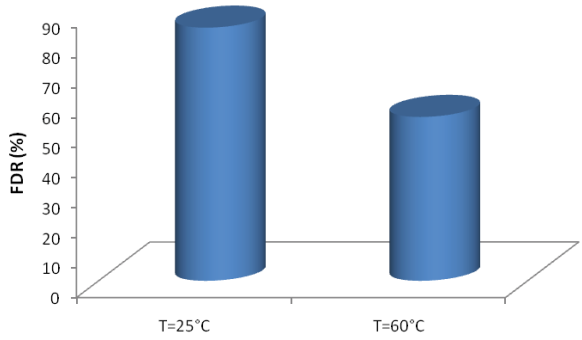

Fig. 5. Calculated flux decay ratios (FDR) with and without heating.

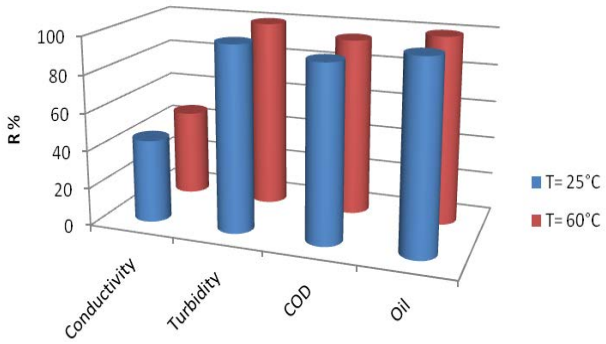

Fig. 6. Retention of different parameters by Sm-Ti/Z 3 membrane at 3 bar.

results from the absence of hydrogen bonding an interaction at the membrane interfaces level and was caused by adsorption. To surmount this obstacle, numerous efforts have been made related to membrane regeneration and results have shown that the cost of ultrafiltration is raised by cleaning process to remove fouling substances [42,43]. Thus, a number of experiments of cleaning process were realized in order to regenerate the membrane, using

Table 1
Composition of the raw and treated effluents using Sm-Ti/Z 3 membrane

	pH	Conductivity (ms/cm)	Oil content (mg/L)	COD (mg/L)	Turbidity (NTU)	Flux (L/h m² bar)
Raw effluent	6.6 ± 0.2	4.97 ± 0.4	40,000 ± 500	6,570 ± 200	3,810 ± 100	–
Permeate Sm-Ti/Z 3 membrane (T = 25°C, P = 3 bar)	7.95 ± 0.2	2.8 ± 0.4	192 ± 10	460 ± 50	65 ± 2	50 ± 2
Permeate Sm-Ti/Z 3 membrane (T = 60°C, P = 3 bar)	7.93 ± 0.2	2.6 ± 0.4	180 ± 10	360 ± 50	2 ± 0.2	146 ± 5

Table 2
Retention of high metal before and after treatment using Sm-Ti/Z 3 membrane

Parameters	Raw effluent (mg/L)	Permeate Sm-Ti/Z 3 membrane (mg/L)	Limits* (mg/L)
Copper	2.631 ± 0.02	0.095 ± 0.002 (TR: 96%)	2
Iron	0.117 ± 0.001	0.117 ± 0.001	10
Plumb	17.05 ± 0.02	0.029 ± 0.002 (TR: 99.82%)	1
Nickel	<0.1 ± 0.001	<0.1 ± 0.001	1
Zinc	4.115 ± 0.02	0.102 ± 0.002 (TR: 97.51%)	5
Chromium	<0.02 ± 0.001	<0.02 ± 0.001	1.5

*: Limits set by Tunisian Environmental Legislation

Table 3
Resistance values of the ultrafiltration membranes

Sample	$R_T \times 10^{12}$ (m^{-1})	$R_m \times 10^{12}$ (m^{-1})	$R_{rev} \times 10^{12}$ (m^{-1})	$R_{irrev} \times 10^{12}$ (m^{-1})
Sm-Ti/Z 3 membrane	14.5 ± 0.5	2.98 ± 0.1	4.8 ± 0.1	6.5 ± 0.1

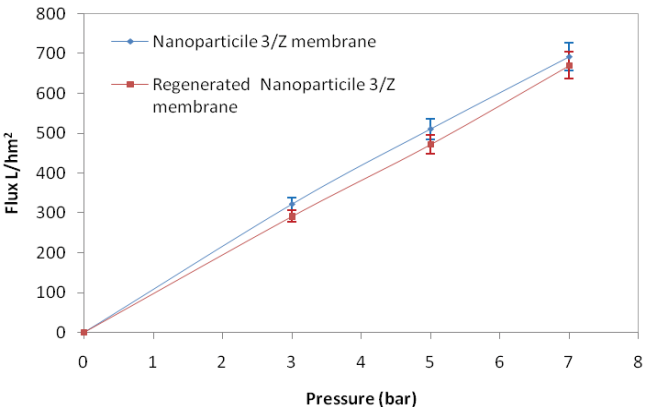

Fig. 7. Permeate flux vs. pressure of unused and regenerated membranes: Sm-Ti/Z 3.

alternatively distillated water, basic solution of NaOH (pH ≈ 8.3), and acidic solution of HNO_3 (pH ≈ 3.5). The efficiency of the regeneration is confirmed when similar permeability of both regenerated and unused membrane was achieved. Fig. 7 shows the evolution of the permeate flux with the TMP of unused and regenerated Sm-Ti/Z 3 membrane. It is clear that both permeability values are very close. This result confirms again the high quality of the prepared membrane.

4. Conclusions

In this work, composite UF ceramic membrane were prepared by deposition of a mixture of TiO_2/Smectite nanocomposite (Sm NC) and commercial TiO_2 nanoparticles (Ti NP) on zeolite support using the layer-by-layer method. The best membrane with a percentage of 70% Sm NC and 30% Ti NP shows a homogenous surface and good adhesion on the support with a filtration layer thickness of 3 μm and a mean pore diameter of 16 nm. The application of Sm-Ti/Z 3 membrane to the purification of the oily effluent contaminated with heavy metal from electroplating industry exhibited a high performances at 60°C with a stabilized permeate flux at 146 L/h m² and almost total retention in terms of turbidity, COD, heavy metals and oil. In particular, an important retention of copper, zinc and plumb of more than 96% was achieved. The efficiency of the membrane regeneration was confirmed by the obtention of similar permabilities of both regenerated and unused membranes.

Acknowledgments

The authors gratefully acknowledge funding from ERANETMED_WATER-13-043 SETPROPER program, research project supported by the European commission and the SOPAL Company.

References

[1] Q. Zhang, N. Liu, Y. Cao, W. Zhang, Y. Wei, L. Feng, L. Jiang, A facile method to prepare dual-functional membrane for efficient oil removal and in situ reversible mercury ions adsorption from wastewater, Appl. Surf. Sci., 434 (2018) 57–62.

[2] H. Boleydei, N. Mirghaffari, O. Farhadian, Comparative study on adsorption of crude oil and spent engine oil from seawater and freshwater using algal biomass, Environ. Sci. Pollut. Res., 25 (2018) 21024–21035.

[3] R. Yang, G. Zhang, S. Li, F. Moazeni, Y. Li, Y. Wu, W. Zhang, T. Chen, G. Liu, B. Zhang, X. Wu, Degradation of crude oil by mixed cultures of bacteria isolated from the Qinghai-Tibet plateau and comparative analysis of metabolic mechanisms, Environ. Sci. Pollut. Res., 26 (2018) 1834–1847.

[4] L. Yu, G. Hao, Q. Liang, S. Zhou, N. Zhang, W. Jiang, Facile preparation and characterization of modified magnetic silica nanocomposite particles for oil absorption, Appl. Surf. Sci., 357 (2015) 2297–2305.

[5] A. Al-Shamrani, A. James, H. Xiao, Separation of oil from water by dissolved air flotation, Colloids Surf., A, 209 (2002) 15–26.

[6] J. Rubio, M.L. Souza, R.W. Smith, Overview of flotation as a wastewater treatment technique, Miner. Eng., 15 (2002) 139–155.

[7] M. Stewart, K. Arnold, Chapter 3 – Produced Water Treating Systems, M. Stewart, K. Arnold, Eds., Emulsions and Oil Treating Equipment: Selection, Sizing and Troubleshooting, Gulf Professional Publishing, 2009, pp. 107–211.

[8] A. Cambiella, J.M. Benito, C. Pazos. J. Coca, Centrifugal separation efficiency in the treatment of waste emulsified oils, Chem. Eng. Res. Des., 84 (2006) 69–76.

[9] R. Zaneti, R. Etchepare, J. Rubio, Car wash wastewater reclamation. Full-scale application and upcoming features, Resour. Conserv. Recycl., 55 (2011) 953–959.

[10] S.W. Puasa, K.N. Ismail, M.A.A. Mahadi, N.M. Zainuddin, M.N.M. Mukelas, Polynomial regression analysis for removal of heavy metal mixtures in coagulation/flocculation of electroplating wastewater, Indonesian J. Chem., 21 (2021) 46–56, doi: 10.22146/ijc.52251.

[11] Jumina, Y. Priastomo, H.R. Setiawan, Mutmainah, Y.S. Kurniawan, K. Ohto, Simultaneous removal of lead(II), chromium(III), and copper(II) heavy metal ions through an adsorption process using C-phenylcalix[4]pyrogallolarene material, J. Environ. Chem. Eng., 8 (2020) 103971, doi: 10.1016/j.jece.2020.103971.

[12] M.H. Sadeghi, M.A. Tofighy, T. Mohammadi, One-dimensional graphene for efficient aqueous heavy metal adsorption: rapid removal of arsenic and mercury ions by graphene oxide nanoribbons (GONRs), Chemosphere, 253 (2020) 126647, doi: 10.1016/j.chemosphere.2020.126647.

[13] D.C. Metcalfe, P. Jarvis, C. Rockey, S. Judd, Pre-treatment of surface waters for ceramic microfiltration, Sep. Purif. Technol., 163 (2016) 173–180.

[14] I.A. Rodriguez Boluarte, M. Andersen, B. Kumar Pramanik, C.-Y. Chang, S. Bagshaw, L. Farago, V. Jegatheesan, L. Shu, Reuse of car wash wastewater by chemical coagulation and membrane bioreactor treatment processes, Int. Biodeterior. Biodegrad., 113 (2016) 44–48.

[15] R. Zolfaghari, A. Fakhru'l-Razi, L.C. Abdullah, S.S.E.H. Elnashaie, A. Pendashteh, Demulsification techniques of water-in-oil and oil-in-water emulsions in petroleum industry, Sep. Purif. Technol., 170 (2016) 377–407.

[16] A. Hong, A.G. Fane, R. Burford, Factors affecting membrane coalescence of stable oil-in-water emulsions, J. Membr. Sci., 222 (2003) 19–39.

[17] U. Daiminger, W. Nitsch, P. Plucinski, S. Hoffmann, Novel techniques for oil/water separation, J. Membr. Sci., 99 (1995) 197–203.

[18] A. El-Kayar, M. Hussein, A.A. Zatout, A.Y. Hosny, A.A. Amer, Removal of oil from stable oil–water emulsion by induced air floatation technique, Sep. Technol., 3 (1993) 25–31.

[19] H. Shokrkar, A. Salahi, N. Kasiri, T. Mohammadi, Prediction of permeation flux decline during MF of oily wastewater using genetic programming, Chem. Eng. Res. Des., 90 (2012) 846–853.

[20] X. Hu, Y. Yu, J. Zhou, Y. Wang, J. Liang, X. Zhang, Q. Chang, L. Song, The improved oil/water separation performance of graphene oxide modified Al_2O_3 microfiltration membrane, J. Membr. Sci., 476 (2015) 200–204.

[21] A. Agi, R. Junin, A.Y.M. Alqatta, A. Gbadamosi, A. Yahya, A. Abbas, Ultrasonic assisted ultrafiltration process for emulsification of oil field produced water treatment, Ultrason. Sonochem., 51 (2018) 214–222.

[22] S. Saki, N. Uzal, Preparation and characterization of PSF/PEI/$CaCO_3$ nanocomposite membranes for oil/water separation, Environ. Sci. Pollut. Res. Int., 25 (2018) 25315–25326.

[23] D. Zhao, C. Su, G. Liu, Y. Zhu, Z. Gu, Performance and autopsy of nanofiltration membranes at an oil-field wastewater desalination plant, Environ. Sci. Pollut. Res., 26 (2019) 2681–2690.

[24] M. Golpour, M. Pakizeh, Development of a new nanofiltration membrane for removal of kinetic hydrate inhibitor from water, Sep. Purif. Technol., 183 (2017) 237–248.

[25] S. Kasemset, A. Lee, D.J. Miller, B.D. Freeman, M.M. Sharma, Effect of polydopamine deposition conditions on fouling resistance, physical properties, and permeation properties of reverse osmosis membranes in oil/water separation, J. Membr. Sci., 425–426 (2013) 208–216.

[26] H. Aloulou, W. Aloulou, M O. Daramola, R. Ben Amar, Silane-grafted sand membrane for the treatment of oily wastewater via air gap membrane distillation: study of the efficiency in comparison with microfiltration and ultrafiltration ceramic membranes, Mater. Chem. Phys., 261 (2021) 124186, doi: 10.1016/j.matchemphys.2020.124186.

[27] J.-H. Ha, S.Z.A. Bukhari, J. Lee, I.-H. Song, C. Park, Preparation processes and characterizations of alumina-coated alumina support layers and alumina-coated natural material-based support layers for microfiltration, Ceram. Int., 42 (2016) 13796–13804.

[28] L. Zhu, M.L. Chen, Y.C. Dong, C.Y.Y. Tang, A.S. Huang, L.L. Li, A low-cost mullite-titania composite ceramic hollow fiber microfiltration membrane for highly efficient separation of oil-in-water emulsion, Water Res., 90 (2016) 277–285.

[29] J.-H. Ha, Y.-H. Park, I.-H. Song, The preparation and pore characteristics of an alumina coating on a diatomite-kaolin composite support layer, J. Ceram. Soc. Jpn., 122 (2014) 714–718.

[30] S.S. Madaeni, H.A. Monfared, V. Vatanpour, A.A. Shamsabadi, E. Salehi, P. Daraei, S. Laki, S.M. Khatami, Coke removal from petrochemical oily wastewater using γ-Al_2O_3 based ceramic microfiltration membrane, Desalination, 293 (2012) 87–93.

[31] Y. Wu, X. Zhang, S. Liu, B. Zhang, Y. Lu, T. Wang, Preparation and applications of microfiltration carbon membranes for the purification of oily wastewater, Sep. Sci. Technol., 51 (2016) 1872–1880.

[32] W. Aloulou, H. Aloulou, A. Jadda, S. Chakraborty, R. Ben Amar, Characterization of an asymmetric ultrafiltration membrane prepared from TiO_2-smectite nanocomposites doped with commercial TiO_2 and its application to the treatment of textile wastewater, Euro-Mediterr. J. Environ. Integr., 5 (2020), doi: 10.1007/s41207-020-0145-6.

[33] W. Aloulou, W. Hamza, H. Aloulou, A. Oun, S. Khemakhem, A. Jada, S. Chakraborty, S. Curcio, R. Ben Amar, Developing of titania-smectite nanocomposites UF membrane over zeolite based ceramic support, Appl. Clay Sci., 155 (2018) 20–29.

[34] H. Aloulou, H. Bouhamed, A. Ghorbel, R. Ben Amar, S. Khemakhem, Elaboration and characterization of ceramic microfiltration membranes from natural zeolite: application to the treatment of cuttlefish effluents, Desal. Water Treat., 95 (2017) 9–17.

[35] M.A. Anderson, M.J. Gieselmann, Q. Xu, Titania and alumina ceramic membranes, J. Membr. Sci., 39 (1988) 243–258.

[36] H. Aloulou, H. Bouhamed, R. Ben Amar, S. Khemakhem, New ceramic microfiltration membrane from Tunisian natural sand: application for tangential wastewater treatment, Desal. Water Treat., 78 (2017) 41–48.

[37] S. Ayadi, I. Jedidi, S. Lacour, S. Cerneaux, M. Cretin, R. Ben Amar, Preparation and characterization of carbon

microfiltration membrane applied to the treatment of textile industry effluents, Sep. Sci. Technol., 51 (2016) 1520–5754.
[38] G. Veréb, P. Kassai, S.E. Nascimben, G. Arthanareeswaran, C. Hodúr, Z. László, Intensification of the ultrafiltration of real oil-contaminated (produced) water with pre-ozonation and/or with TiO_2, TiO_2/CNT nanomaterial-coated membrane surfaces, Environ. Sci. Pollut. Res., 27 (2020) 22195–22205.
[39] B. Tansel, W.-Y. Bao, I.N. Tansel, Characterization of fouling kinetics in ultrafiltration systems by resistances in series model, Desalination, 129 (2000) 7–14.
[40] B. Van der Bruggen, G. Cornelis, C. Vandecasteele, I. Devreese, Fouling of nanofiltration and ultrafiltration membranes applied for wastewater regeneration in the textile industry, Desalination, 175 (2005) 111–119.
[41] E. Cornelissen, A. van den Boomgaard, H. Strathmann, Physicochemical aspects of polymer selection for ultrafiltration and microfiltration membranes, J. Membr. Sci., 138 (1998) 283–289.
[42] S. Bousbih, E. Errais, F. Darragi, J. Duplay, M. Trabelsi-Ayadi, M.O. Daramola, R. Ben Amar, Treatment of textile wastewater using monolayered ultrafiltation ceramic membrane fabricated from natural kaolin clay, Environ. Technol., 42 (2019) 3348–3359.
[43] W.L. Han, H.P. Gregor, E.M. Pearce, Interaction of proteins with ultrafiltration membranes: development of a nonfouling index test, J. Appl. Polym. Sci., 77 (2000) 1600–1606.